N73 32375

NASA TECHNICAL MEMORANDUM

NASA TM X-71442

NASA TM X-71442

BALL MOTION AND SLIDING FRICTION IN AN ARCHED OUTER RACE BALL BEARING

by Bernard J. Hamrock
Lewis Research Center
Cleveland, Ohio

TECHNICAL PAPER proposed for submittal to ASME for presentation at the ASME-ASLE Joint Lubrication Conference, Montreal, Quebec, Canada, October 8-10, 1974

Ball Motion and Sliding Friction in an Arched Outer Race Ball Bearing

by Bernard J. Hamrock

Lewis Research Center

Abstract

The motion of the ball and sliding friction in an arched outer-race ball bearing under thrust load is determined. Fatigue life evaluations were made. The analysis is applied to a 150 millimeter bore ball bearing.

The results indicated that for high speed-light load applications the arched bearing has significant improvement in fatigue life over that of a conventional bearing. An arching of 0.254 mm (0.01 in.) was found to be an optimal. For an arched bearing it was also found that a considerable amount of spinning occurs at the outer race contacts.

E-7607

Technical Paper proposed for submittal to ASME for presentation at the ASME-ASLE Joint Lubrication Conference, Montreal, Quebec, Canada, October 8-10, 1974

Symbols

A	distance between raceway groove curvature centers
$\mathcal{A}$	life-side-outer-race curvature center
a	semimajor axis of projected contact ellipse
B	$f_o + f_i - 1 = A/D$
$\mathcal{B}$	ball center initially
b	semiminor axis of projected contact ellipse
$\mathcal{C}$	initial position, inner-raceway groove curvature center
c	inner race bore
D	ball diameter
$\mathcal{D}$	right-side-outer-race curvature center
d	raceway diameter
d_m	pitch diameter initially
$\overline{d_m}$	pitch diameter after dynamic effects have acted on the ball
E	defined by equation (65)
$e_1, e_2, \ldots, e_7$	defined by equations (55), (56), (57), (58), (60), (61), and (62)
F	force
F_a	axially applied load
f	r/D
$\mathcal{H}$	inner race contact-initially
g	amount of arching, or width of material removed from outer race of conventional bearing
$\mathcal{H}$	left outer-race contact, initially

h	distance from top of arch to top of ball when bearing is in radial contact position
I_P	polar moment of inertia of ball
$\mathcal{I}$	inner-race contact finally
J	Jacobian defined by equation (64)
$\mathcal{J}$	left-outer-race contact, finally
K	load-deflection constant
$\mathcal{K}$	right-outer-race contact, finally
k	a/b
L	life in hours
$\mathcal{L}$	ball center, finally
M	frictional moments
$\overline{M}$	inertia moments
$\mathcal{M}$	final position, inner-raceway groove curvature center
m	ball mass
$\mathcal{N}$	tip of arch
n	rotational speed
P_d	bearing diametral clearance
P_e	free end play
Q	ball normal load
R	radius of deformed pressure surface in plane of major axis of pressure ellipse
r	raceway groove curvature radius

$\bar{r}$	$\sqrt{R^2 - x^2} - \sqrt{R^2 - a^2} + \sqrt{\left(\frac{D}{2}\right)^2 - a^2}$
r'	effective rolling radius of ball
S_d	diametral play
S_x	axial distance between the final position of the inner and left outer raceway groove curvature center
S_z	radial distance between the final position of the inner-raceway groove curvature center and the right or left outer raceway groove curvature center
U', V', W' X, Y, Z x, y, z x', y', z'	coordinate systems defined in report
V	radial projection of distance between ball center and outer-raceway groove curvature center
W	axial projection of distance between ball center and outer-raceway groove curvature center
Z	number of balls
α	radial contact angle
α', β'	angles defining direction of ω_B
β	axial contact angle, initially
Δ	distance between raceway groove curvature center and final position of ball center
δ	contact deformation
δ_a	axial displacement

η defined by equation (10)

Λ density

λ modulus of elasticity
ξ Poisson's ratio
Ω absolute angular velocity

Ω_c orbital angular velocity of balls about the bearing axis

ω relative angular velocity

ω_B angular velocity of ball about its center

Subscripts

i inner race

o outer race

ol outer left

or outer right

R rolling

S spinning

x'X
y'Y
z'Z
} coordinate system defined in report

Introduction

Aircraft gas turbine engine rotor bearings currently operate in the speed range from 1.5 to 2.0 million DN (bearing bore in mm times shaft speed in rpm). It is estimated that engine designs of the next decade will require bearings to operate at DN values of 3 million or more (ref. 1). In this DN range, analyses (refs. 2 and 3) predict a prohibitive reduction in bearing fatigue life due to the high centrifugal forces developed between the rolling elements and the outer race.

An approach to the high speed-bearing problem is an arched outer race ball bearing. In this bearing, when centrifugal forces become large, the contact load is shared by two outer race contacts instead of just one outer race contact as is present in conventional ball bearings. A first order thrust load analysis of an arched-outer-race ball bearing that considers centrifugal forces but that neglects gyroscopics, elastohydrodynamics, and sliding friction was performed (ref. 4, 5). The analysis was applied to a 150-millimeter-bore, angular-contact ball bearing. The results indicated that an arched bearing is highly desirable for high speed applications. In particular, for a DN value of 3 million (20 000 rpm) and an applied axial load of 4450 newtons (1000 lbs), an arched bearing shows an improvement in life of 306% over that of a conventional bearing.

The objective of the work described in this paper was to conduct fatigue life analysis of the arched outer race ball bearing while considering the complete motion of the ball as well as the sliding friction. A comparison will be made with a conventional ball bearing as well as comparing the results of ref. 4 and 5 (where only centrifugal force was considered). A more detailed report of the above is given by the author in ref. 6. The analysis in this paper will neglect elastohydrodynamics and thermal effects. Furthermore, the approach to be used is that used by Jones (ref. 2) in analyzing a conventional ball bearing.

Arched-Bearing Geometry

Figure 1 shows how the arched outer race is made. A conventional outer race is shown in figure 1(a) with a race radius of r_o. Also shown

in figure 1(a) is the portion of the conventional outer race that is removed in forming an arched outer race. Figure 1(b) shows the arched outer race with the portion of length g removed. Note that there are now two outer-race radius centers separated by a distance g. With modern technology being what it is, an arched outer race can be in one piece.

Figure 2 shows the arched bearing while in a noncontacting position. Here the pitch diameter d_m, diametral clearance P_d, diametral play S_d, and raceway diameters d_i and d_o are defined. The diametral play is the total amount of radial movement allowed in the bearing. Furthermore, the diametral clearance is the diametral play plus two times the distance from the bottom of the ball to the tip of the arch when the bearing is in a radial contact position.

Figure 3 shows the arched bearing in a radial contact position. Instead of contacting at one point at the bottom of the outer raceway, the ball contacts at two points separated by an angle 2α. From figure 3 the radial contact angle α can be written as

$$\alpha = \sin^{-1}\left(\frac{g}{2r_o - D}\right) \tag{1}$$

A distance which needs to be formulated is the distance from the tip of the arch to the bottom of the ball when the ball and raceway are in the radial contact position as shown in figure 3. This distance is defined as h. From figure 3(b) and using the Pythagorian theorem to solve for h the following can be written:

$$h = -\frac{D}{2} - \left(r_o - \frac{D}{2}\right)\cos\alpha + \frac{1}{2}\left[D(4r_o - D) + (2r_o - D)^2\cos^2\alpha\right]^{1/2} \tag{2}$$

Note that, as one might expect, as $\alpha \to 0^o$, $h \to 0$. With h known, a number of conventional bearing parameters can be formulated from figures 2 and 3. The outer-raceway diameter may be written as

$$d_o = \bar{d}_i + P_d + 2D \tag{3}$$

$$P_d = S_d + 2h \tag{4}$$

where $\bar{d}_i$ is the inner raceway diameter after centrifugal growth has been considered. Using the centrifugal growth equation found in Timoshenko (ref. 7) the inner raceway diameter will expand according to the following formulation:

$$\bar{d}_i = d_i + \frac{\Lambda d_i}{1544\lambda_i}\left(\frac{n_i\pi}{30}\right)^2\left[\left(\frac{d_i}{2}\right)^2(1 - \xi_i) + \left(\frac{c}{2}\right)^2(3 + \xi_i)\right] \tag{5}$$

From equations (3) and (4) the diametral play can be written as:

$$S_d = d_o - \bar{d}_i - 2D - 2h \tag{6}$$

The pitch diameter d_m from figure 2 can be expressed as:

$$d_m = \bar{d}_i + \frac{S_d}{2} + D \tag{7}$$

Figure 4 shows the arched bearing while in the axial position. From this figure the distance between the center of curvature of the

inner and left outer race can be written as:

$$A = r_o + r_i - D$$

With $f_o = r_o/D$ and $f_i = r_i/D$ the above equation becomes

$$A = BD \tag{8}$$

where

$$B = f_o + f_i - 1 \tag{9}$$

From figure 4(b) the following equation can be written:

$$\eta = r_o - \sqrt{r_o^2 - \left(\frac{g}{2}\right)^2} \tag{10}$$

With η known, the contact angle can be expressed as:

$$\beta = \cos^{-1}\left(\frac{A - \frac{P_d}{2} - \eta}{A}\right) \tag{11}$$

The end play of an arched bearing is:

$$P_e = 2A \sin \beta - g \tag{12}$$

Contact Geometry

From the experimental work of Haines and Edmonds (ref. 8) it is observed that the arched bearing will initially operate with two point

contact at the lower speeds and then with three-point contact at higher speeds when the centrifugal forces become significant. When centrifugal force acts on the ball, the inner and outer-raceway contact angles are dissimilar; therefore, the lines of action between raceway groove curvature radius centers become discontinuous, as shown in figure 5. In this figure the left and right-outer raceway groove curvature centers a and $\mathcal{N}$ are fixed in space and the inner-raceway groove curvature center c moves axially relative to those fixed centers.

Figure 5 gives the distance between the fixed right and left-outer raceway groove curvature centers a or $\mathcal{N}$ and the final position of the ball center $\mathcal{L}$ as:

$$\Delta_{ol} = r_o - \frac{D}{2} + \delta_{ol} = (f_o - 0.5)D + \delta_{ol} \tag{13}$$

$$\Delta_{or} = (f_o - 0.5)D + \delta_{or} \tag{14}$$

where

δ_{ol} normal contact deformation at left-outer raceway center

δ_{or} normal contact deformation at right-outer raceway center

Similarly, the distance between the final inner-raceway groove curvature center m and the final position of the ball center $\mathcal{L}$ is:

$$\Delta_i = (f_i - 0.5)D + \delta_i \tag{15}$$

where δ_i is the normal contact deformation at the inner-raceway center.

The axial distance between the final position of the inner and left-outer-raceway groove curvature center is:

$$S_x = A \sin \beta + \delta_a \tag{16}$$

where δ_a is the axial displacement. The radial distance between the final position of the inner-raceway groove curvature center and the right or left-outer-raceway groove curvature center is:

$$S_z = A \cos \beta \tag{17}$$

From figure 5 and equations (13) to (17) the following can be written:

$$\beta_{or} = \sin^{-1}\left[\frac{g - W}{(f_o - 0.5)D + \delta_{or}}\right] \tag{18}$$

$$\beta_{ol} = \sin^{-1}\left[\frac{W}{(f_o - 0.5)D + \delta_{ol}}\right] \tag{19}$$

$$\beta_i = \sin^{-1}\left[\frac{A \sin \beta + \delta_a - W}{(f_i - 0.5)D + \delta_i}\right] \tag{20}$$

Using the Pythagorean theorem and regrouping terms results in:

$$\delta_{or} = \sqrt{V^2 + (g - W)^2} - D(f_o - 0.5) \tag{21}$$

$$\delta_{ol} = \sqrt{V^2 + W^2} - D(f_o - 0.5) \tag{22}$$

$$\delta_i = \sqrt{(A \cos \beta - V)^2 + (A \sin \beta + \delta_a - W)^2} - D(f_i - 0.5) \qquad (23)$$

The normal loads are related to the normal contact deformation in the following way:

$$Q = K\delta^{1.5} \qquad (24)$$

With the proper subscripting of i, oℓ, and or this equation could represent the normal loads of the inner ring Q_i, left outer ring $Q_{o\ell}$, or right outer ring Q_{or}. Having defined the normal load in terms of the load deflection constant, one needs next to know the equations for the load deflection constants. The derivation of the load deflection constants will not be derived here but can be obtained from refs. 5, 6, or 7.

Figure 6 shows the position of the ball and raceway groove curvature centers and contacts with and without dynamic effects acting on the ball. In this figure the unbarred values represent initial location and the barred values represent final location when dynamic effects have acted on the ball. From this figure the pitch diameter when dynamic effects have acted on the ball is:

$$\bar{d}_m = d_m + 2\left[(f_o - 0.5)D + \delta_{o\ell}\right] \cos \beta_{o\ell} - 2(f_o - 0.5)D \cos \beta \qquad (25)$$

One design constraint which needs to be adhered to is for the left and right outer race contacts NOT to overlap. The following inequality must be satisfied in order to prevent overlapping of the left and right outer race contact:

$$a_{o\ell} \cos \beta_{o\ell} + a_{or} \cos \beta_{or} < \frac{D}{2} (\sin \beta_{o\ell} + \sin \beta_{or}) \qquad (A)$$

If the above inequality is not satisfied, then by increasing the amount of arching one can get the inequality to be satisfied.

Inertia Forces and Moments on Ball

As was mentioned in the introduction, the analysis which follows is that of Jones (ref. 2) with the exception that Jones analyzes a conventional bearing and in this paper an arched outer race ball bearing is analyzed.

Figure 7 shows the instantaneous position of an element of ball mass of a high speed, ball bearing. From Jones (ref. 2) the equations for the inertia forces and moments on the ball can be written as:

$$F_{x'} = 0 \qquad (26)$$

$$F_{y'} = 0 \qquad (27)$$

$$F_{z'} = m\left(\frac{\overline{d}_m}{2}\right) \Omega_c^2 \qquad (28)$$

$$\overline{M}_{x'} = 0 \qquad (29)$$

$$\overline{M}_{y'} = I_P \omega_B \Omega_c \sin \alpha' \qquad (30)$$

$$\overline{M}_{z'} = -I_P \omega_B \Omega_c \cos \alpha' \sin \beta' \qquad (31)$$

where

$\omega_B = \dot{\theta}$ = angular velocity of ball about its center

$\Omega_c = \dot{\varphi}$ = angular velocity of balls about bearing axis

m = mass of ball

I_P = polar moment of inertia of ball

From figure 7 the following equations can be written:

$$\left.\begin{aligned} \omega_{x'} &= \omega_B \cos \alpha' \cos \beta' \\ \omega_{y'} &= \omega_B \cos \alpha' \sin \beta' \\ \omega_{z'} &= \omega_B \sin \alpha' \end{aligned}\right\} \tag{32}$$

Relative Motions of Rolling Elements

According to Hertz the radius of the deformed pressure surface in the plane of the major axis of the pressure ellipse is:

$$R = \frac{2fD}{2f + 1} \tag{33}$$

Figure 8 shows the contact of the ball with the right outer race. Due to $\omega_o \cos \beta_{or}$ a point (x_{or}, y_{or}) on the right outer race has the linear velocity V'_{lor} or

$$V'_{lor} = - \frac{\bar{d}_m \omega_o}{2} - \bar{r}_{or} \omega_o \cos \beta_{or} \tag{34}$$

where

$$\bar{r}_{or} = \sqrt{R_o^2 - X_{or}^2} - \sqrt{R_o^2 - a_{or}^2} + \sqrt{\left(\frac{D}{2}\right)^2 - a_{or}^2} \tag{35}$$

Due to $\omega_{x'} \cos \beta_{or}$ and $\omega_{z'} \sin \beta_{or}$ a point (X_{or}, Y_{or}) on the ball has the linear velocity V'_{2or}, where

$$V'_{2or} = \bar{r}_{or}(\omega_{z'} \sin \beta_{or} - \omega_{x'} \cos \beta_{or}) \tag{36}$$

The velocity with which the right outer race slips on the ball in the $\bar{Y}$ direction is

$$V'_{Yor} = V'_{10r} - V'_{2or}$$

Substituting equations (34) and (36) into the above equation while making use of equation (32) gives:

$$V'_{Yor} = -\frac{\bar{d}_m \omega_o}{2}$$

$$+ \bar{r}_{or} \omega_o \left[\frac{\omega_B}{\omega_o} (\cos \alpha' \cos \beta' \cos \beta_{or} - \sin \alpha' \sin \beta_{or}) - \cos \beta_{or}\right] \tag{37}$$

Due to $\omega_{y'}$ all points within the pressure area have a velocity of slip of race on the ball of V'_{xor} in the x'-z' plane.

$$V'_{Xor} = -\omega_{y'} \bar{r}_{or} = -\omega_B \bar{r}_{or} \cos \alpha' \sin \beta' \tag{38}$$

Due to the components of velocity which lie along the line defined by β_{or} there is a spin of the right outer race, ω_{Sor} with respect to

the ball. Due to component $\omega_o \sin \beta_{or}$ the following can be written:

$$\omega_{1or} = \omega_o \sin \beta_{or} \tag{39}$$

Due to the components ω_x, $\sin \beta_{or}$ and ω_z, $\cos \beta_{or}$ the following can be written:

$$\omega_{2or} = \omega_x, \sin \beta_{or} + \omega_z, \cos \beta_{or} \tag{40}$$

Therefore the spin of the right outer race with respect to the ball can be written as:

$$\omega_{Sor} = \omega_{1or} - \omega_{2or}$$

Substituting equations (39) and (40) into the above equation while making use of equation (32) gives

$$\omega_{Sor} = \omega_o \left[\sin \beta_{or} - \frac{\omega_B}{\omega_o} (\cos \alpha' \cos \beta' \sin \beta_{or} + \sin \alpha' \cos \beta_{or}) \right] \tag{41}$$

Making use of figure 8 and equation (32) one finds the angular velocity of roll of the ball on the outer-right race contact to be

$$\omega_{Ror} = \omega_o \left[-\cos \beta_{or} + \frac{\omega_B}{\omega_o} (\cos \alpha' \cos \beta' \cos \beta_{or} - \sin \alpha' \sin \beta_{or}) \right] \tag{42}$$

In a similar manner the following equations can be written for the outer left and inner contacts:

$$V'_{Yol} = -\frac{\bar{d}_m \omega_o}{2} + \bar{r}_{ol}\omega_o\left[\frac{\omega_B}{\omega_o}\sin\alpha'\sin\beta_{ol} + \frac{\omega_B}{\omega_o}\cos\alpha'\cos\beta'\cos\beta_{ol} - \cos\beta_{ol}\right] \tag{43}$$

$$V'_{Xol} = -\left(\frac{\omega_B}{\omega_o}\right)\bar{r}_{ol}\omega_o\cos\alpha'\sin\beta' \tag{44}$$

$$\omega_{Sol} = \omega_o\left[\frac{\omega_B}{\omega_o}\cos\alpha'\cos\beta'\sin\beta_{ol} - \frac{\omega_B}{\omega_o}\sin\alpha'\cos\beta_{ol} - \sin\beta_{ol}\right] \tag{45}$$

$$\omega_{Rol} = \omega_o\left[-\cos\beta_{ol} + \frac{\omega_B}{\omega_o}(\cos\alpha'\cos\beta'\cos\beta_{ol} + \sin\alpha'\sin\beta_{ol})\right] \tag{46}$$

$$V'_{Yi} = -\frac{\bar{d}_m\omega_i}{2} + \bar{r}_i\omega_i\left[\cos\beta_i - \frac{\omega_B}{\omega_i}(\cos\alpha'\cos\beta'\cos\beta_i + \sin\alpha'\sin\beta_i)\right] \tag{47}$$

$$V'_{Xi} = -\frac{\omega_B}{\omega_i}\bar{r}_i\omega_i\cos\alpha'\sin\beta' \tag{48}$$

$$\omega_{Si} = \omega_i\left[\sin\beta_i + \frac{\omega_B}{\omega_i}(\sin\alpha'\cos\beta_i - \cos\alpha'\cos\beta'\sin\beta_i)\right] \tag{49}$$

$$\omega_{Ri} = \omega_i\left[\cos\beta_i - \frac{\omega_B}{\omega_i}(\cos\alpha'\cos\beta'\cos\beta_i + \sin\alpha'\sin\beta_i)\right] \tag{50}$$

There are some radii denoted as r'_{ol}, r'_{or}, and r'_i for the outer left, outer right, and inner contacts, respectively, called the effective rolling radii at which pure rolling occurs. These radii are not necessarily restricted to points which lie on the deformed pressure surfaces if gross slip between the ball and races occurs. At these effective rolling radii r'_{ol}, r'_{or}, and r'_i on the ball, the translational velocity of ball and race is the same. Therefore the following equations can be written:

$$\frac{\omega_B}{\omega_o} = \frac{\frac{\bar{d}_m}{2r'_{ol}} + \cos\beta_{ol}}{\cos\alpha' \cos\beta' \cos\beta_{ol} + \sin\alpha' \sin\beta_{ol}} \tag{51}$$

$$\frac{\omega_B}{\omega_o} = \frac{\frac{\bar{d}_m}{2r'_{or}} + \cos\beta_{or}}{\cos\alpha' \cos\beta' \cos\beta_{or} - \sin\alpha' \sin\beta_{or}} \tag{52}$$

$$\frac{\omega_B}{\omega_i} = \frac{-\frac{\bar{d}_m}{2r'_i} + \cos\beta_i}{\cos\alpha' \cos\beta' \cos\beta_i + \sin\alpha' \sin\beta_i} \tag{53}$$

From equation (52) solving for r'_{or} the following can be written:

$$r'_{or} = \frac{\frac{\bar{d}_m}{2}}{\frac{\omega_B}{\omega_o}(\cos\alpha' \cos\beta' \cos\beta_{or} - \sin\alpha' \sin\beta_{or}) - \cos\beta_{or}} \tag{54}$$

If instead of the ball center being fixed in space the outer race is fixed, then the ball center must orbit about the center of the fixed coordinate system with an angular speed of $\Omega_i = -\omega_o$. Therefore the inner race must rotate with an absolute angular speed of $\Omega_i = \omega_i + \Omega_i$. Using these relationships the relative angular speeds ω_o and ω_i can be described in terms of the absolute angular speed of the inner raceway.

The equations for the friction forces (F_Y and F_X) and moments (M_S, $M_{y'}$, and M_R) can be found in Jones (ref. 2).

Equilibrium Conditions

Figure 9 shows the moments acting on the ball. From this figure the following equations can be written.

$$e_1 = -M_{Rol} \sin \beta_{ol} + M_{Sol} \cos \beta_{ol} + \overline{M}_{z'} + M_{Ri} \sin \beta_i - M_{Si} \cos \beta_i + M_{Ror} \sin \beta_{or} + M_{Sor} \cos \beta_{or} = 0 \tag{55}$$

$$e_2 = -M_{Rol} \cos \beta_{ol} - M_{Sol} \sin \beta_{ol} + M_{Ri} \cos \beta_i + M_{Si} \sin \beta_i - M_{Ror} \cos \beta_{or} + M_{Sor} \sin \beta_{or} = 0 \tag{56}$$

$$e_3 = \overline{M}_{y'} - M_{y'ol} - M_{y'or} - M_{y'i} = 0 \tag{57}$$

Figure 10 shows the forces acting on the ball. From this figure the following equations can be written.

$$e_4 = -Q_{ol} \cos \beta_{ol} - F_{xol} \sin \beta_{ol} - Q_{or} \cos \beta_{or} + F_{xor} \sin \beta_{or} + F_{z'} + Q_i \cos \beta_i + F_{xi} \sin \beta_i = 0 \tag{58}$$

$$e_5 = Q_{ol} \sin \beta_{ol} - F_{xol} \cos \beta_{ol} - Q_{or} \sin \beta_{or}$$

$$- F_{xor} \cos \beta_{or} - Q_i \sin \beta_i + F_{xi} \cos \beta_i = 0 \qquad (59)$$

$$e_6 = F_{Yol} + F_{Yor} + F_{Yi} = 0 \qquad (60)$$

Ball bearings subject to a pure thrust load have the following relationship.

$$e_7 = Q_i \sin \beta_i - F_{xi} \cos \beta_i - \frac{F_a}{Z} = 0 \qquad (61)$$

Note that because of equation (61) equation (59) can be rewritten as

$$e_5 = Q_{ol} \sin \beta_{ol} - F_{xol} \cos \beta_{ol} - Q_{or} \sin \beta_{or} - F_{xor} \cos \beta_{or} - \frac{F_a}{Z} = 0 \qquad (62)$$

Therefore we have seven equations (55), (56), (57), (58), (60), (61), and (62) and seven unknowns V, W, δ_a, α', β', r'_{ol}, and r'_i.

The numerical iteration procedure of the seven simultaneous nonlinear equations is given in detail in ref. 6. The resulting iteration equation is the following

$$\begin{bmatrix} V \\ W \\ \vdots \\ r'_i \end{bmatrix} = \begin{bmatrix} \overline{V} \\ \overline{W} \\ \vdots \\ \overline{r}'_i \end{bmatrix} - \left[\begin{array}{c|c} J^{-1} & \\ \hline & \overline{V}, \overline{W}, \ldots \overline{r}'_i \end{array}\right] \begin{bmatrix} e_1(\overline{V}, \overline{W}, \ldots, \overline{r}'_i) \\ e_2(\overline{V}, \overline{W}, \ldots, \overline{r}'_i) \\ \vdots \\ e_7(\overline{V}, \overline{W}, \ldots, \overline{r}'_i) \end{bmatrix} \qquad (63)$$

where

$$J = \begin{bmatrix} \frac{\partial e_1}{\partial V} & \frac{\partial e_1}{\partial W} & \cdots & \frac{\partial e_1}{\partial r_i'} \\ \frac{\partial e_2}{\partial V} & \frac{\partial e_2}{\partial W} & \cdots & \frac{\partial e_2}{\partial r_i'} \\ \cdot & \cdot & \cdots & \cdot \\ \cdot & \cdot & \cdots & \cdot \\ \cdot & \cdot & \cdots & \cdot \\ \frac{\partial e_7}{\partial V} & \frac{\partial e_7}{\partial W} & \cdots & \frac{\partial e_7}{\partial r_i'} \end{bmatrix} \tag{64}$$

and $\overline{V}$, $\overline{W}$, . . . , $\overline{r}_i'$ are initial estimates of V, W, . . . , r_i'.

Therefore from the iterative method described, one is able to obtain values of V, W, δ_a, α', β', r_{ol}', and r_i' which satisfy equations (55), (56), (57), (58), (60), (61), and (62). With V, W, δ_a, α', β', r_{ol}', and r_i' known and given equations (18), (19), (20), and (24) the contact loads Q_i, Q_{ol}, and Q_{or} and contact angles β_i, β_{ol}, and β_{or} can be evaluated and then the fatigue life can be determined. The fatigue life analysis is the same as that presented in refs. 4, 5, or 6 and will not be repeated here. The equations for a conventional bearing can be directly obtained from the arched-bearing analysis by simply letting the amount of arching be zero (g = 0) and not considering equations related to the right outer race.

Discussion of Results

A conventional 150 millimeter ball thrust bearing operating under pure thrust load was used for the computer evaluation. Bearing param-

eters and results such as life, contact loads, contact angles, spin to roll ratio, cage to shaft speed ratio, and maximum compressive stress are shown in Tables 1 through 4. For a given applied axial load and a given inner ring speed the amount of diametrial play S_d (fig. 2) was held fixed while considering different amounts of arching. In an arched bearing the free contact angle β becomes larger than that of the conventional bearing even though the diametrial play is held constant. The greater the amount of arching (the larger the g), the higher the free contact angle.

The following observations can be made from the results in tables 1 to 4:

1. For high speed-light loads there is substantial increase in life for an arched bearing compared to a conventional bearing.
2. An optimal amount of arching when considering fatigue life is 0.254 mm (0.010 in.) for axial applied load of 4450 N (1000 lb) and 0.381 mm (0.015 in.) for axial applied load of 22 200 N (5000 lb). However, these are not strong optimals.
3. At shaft speed equal to 12 000 rpm the arch bearing has made contact with the outer right race.
4. As the amount of arching is increased the outer race spin to roll ratio increases significantly. Therefore for an axial applied load of 22 200 N (5000 lb) one might change the optimal amount of arching to 0.254 mm (0.010 in.).
5. For a conventional bearing the spin to roll ratio of the inner race contact is at least a magnitude larger than that of the outer

race contact. However, for an arched bearing the spin to roll ratios are of the same order for the various contacts.

6. There is less advantage in using an arched bearing at high loads.

In trying to choose the best amount of arching to use, one is confronted with the following constraints:

a. The amount of arching must be large enough so that overlapping of the left and right outer race contacts does not occur. That is, inequality (A) is satisfied. For example, for the bearing considered $0 < g \leq 0.127$ mm (0.005 in.) did not satisfy inequality (A).

b. With arching greater than 0.381 mm (0.015 in.) there can be an order of magnitude more spinning occurring at the outer race contacts.

Therefore, in view of the above, an amount of arching equal to 0.254 mm (0.01 in.) is the best when considering fatigue life and amount of spinning.

Figure 11 shows the effect of speed on outer race normal ball load Q_o, for an arched bearing and a conventional bearing. The axial applied load is fixed at 4450 N (1000 lb). It is seen how the arched outer race shares the load between the left and right outer race contact. As the speed is increased and more centrifugal force acts on the ball it is seen in this figure that the value of the normal ball load for a conventional bearing is considerably higher than the left or right outer race normal ball load of an arch bearing. The result of reducing the outer race normal load from one large load to two smaller loads results in life improvement for the arch bearing.

Figure 12 shows the fatigue life percent of improvement for an arched bearing over that of a conventional bearing for axial applied loads of 4450 and 22 200 N (1000 and 5000 lb). A comparison is also shown between the present results and those of ref. 4 and 5 where only the centrifugal force is considered. The ordinate E of figure 12 is defined by the following:

$$E = \frac{(L|_{g=0.254mm} - L|_{g=0})100}{L|_{g=0}} \tag{65}$$

Figure 12 shows the fatigue life improvement over the conventional bearing is significant for high speed light load condition. This increase is because the load is shared by the two outer race contacts. Furthermore, this figure shows that there is little difference between the fatigue life analyses of this paper and that of ref. 4 and 5.

Figure 13 shows the effect of speed on the absolute value of spin to roll ratio for an arch bearing and a conventional bearing. The applied load is held fixed at 4450 N (1000 lb). This figure shows that for an arched bearing, the outer race spin to roll ratio of the arched bearing is an order of magnitude larger than that of a conventional bearing. Therefore, one might speculate that there is more heat generated in an arch bearing.

Conclusion

The motion of the ball and sliding friction in an angular contact arched-outer-race ball bearing under thrust load is analyzed. This

motion of the ball and sliding friction is expressed in terms of the inertia effects on the ball and the frictional resistance resulting from interfacial slip at the contact areas. The solution of seven simultaneous equations involving double integrals for which closed form solution cannot be found is required. Fatigue life evaluations via Lundberg-Palmgren were made. The similar analysis of a conventional bearing can be directly obtained from the arched bearing analysis by simply letting the amount of arching be zero and not considering equations related to the unloaded half of the outer race. The analysis is applied to a 150 millimeter bore angular contact ball bearing.

The results indicated that for high speed-light load applications the arched outer race ball bearing has significant improvement in fatigue life over that of a conventional bearing. An arching of 0.254 mm (0.01 in.) was found to be an optimal when spinning is considered with fatigue life. For an arched bearing it was also found that a considerable amount of spinning occurs at the outer race contacts.

REFERENCES

1. Brown, P. F., "Bearings and Dampers for Advanced Jet Engines," SAE Paper 700318 (1970).
2. Jones, A. B., "Ball Motion and Sliding Friction in Ball Bearings," J. Basic Eng., 81, 1 (1959).
3. Harris, T. A., "An Analytical Method to Predict Skidding in Thrust-Loaded, Angular-Contact Ball Bearings," J. Lub. Tech., 93, 17 (1971).

4. Hamrock, B. J., and Anderson, W. J., "Analysis of an Arched Outer-Race Ball Bearing Considering Centrifugal Forces," J. Lub. Tech., 95 (1973).

5. Hamrock, B. J., and Anderson, W. J., "Arched-Outer-Race Ball-Bearing Analysis Considering Centrifugal Forces," NASA TN D-6765 (1972).

6. Hamrock, B. J., "Ball Motion and Sliding Friction in an Arched Outer Race Ball Bearing," Proposed NASA Technical Note.

7. Timoshenko, S., Theory of Elasticity, McGraw-Hill, New York, 1934, pp. 63-68.

8. Haines, D. J., and Edmonds, M. J., "A New Design of Angular Contact Ball Bearing," Proc. Inst. Mech. Eng., 195, 382 (1970-1971).

TABLE 1. - CHARACTERISTICS OF A CONVENTIONAL BEARING (g = 0), FOR AN AXIAL APPLIED LOAD OF 4448 N (1000 LB) and 22 241 N (5000 LB)

[Inner-raceway groove curvature, 0.54; outer-raceway groove curvature, 0.52; pitch diameter, 187.55 mm (7.3838 in.); ball diameter, 22.23 mm (0.8750 in.); diametral play, 0.2499 mm (0.0098 in.); 22 balls.]

Rotational speed of inner raceway, n_i, rpm	Axially applied load, F_a, 4448 N (1000 lb)				Axially applied load, F_a, 22 241 N (5000 lb)			
	12 000	16 000	20 000	24 000	12 000	16 000	20 000	24 000
Life, L, hr	12 496	2291	583	192	806	378	155	59
Inner-raceway load, Q_r, N	419.7	452.9	518.5	708.2	2117	2211	2435	2903
Left-outer raceway load, Q_{ol}, N	1844	2995	4403	5849	3406	4577	6164	8226
Right-outer raceway load, Q_{or}, N								
Inner-raceway contact angle, β_r, deg	28.94	26.60	23.00	19.02	29.17	27.71	24.88	20.58
Left-outer raceway contact angle, β_{ol}, deg	4.95	3.08	1.97	1.48	14.93	10.72	7.79	5.86
Right-outer raceway contact angle, β_{or}, deg								
Inner-raceway spin to roll ratio, ω_{cr}/ω_{Ri}	0.4804	0.4625	0.3949	0.3339	0.3620	0.3888	0.3677	0.3109
Left-outer raceway spin to roll ratio, $\omega_{Sol}/\omega_{Rol}$	0.0148	0.0148	0.0027	0.0024	0.0575	0.0455	0.0330	0.0295
Right-outer raceway spin to roll ratio, $\omega_{Sor}/\omega_{Ror}$								
Cage to shaft speed ratio, Ω_c/Ω_i	0.4693	0.4672	0.4605	0.4553	0.4578	0.4596	0.4574	0.4522
Inner-raceway maximum compressive stress, σ_{Mi}, N/cm^2	1.013×10^9	1.040×10^9	1.090×10^9	1.212×10^9	1.737×10^9	1.764×10^9	1.824×10^9	1.937×10^9
Left outer-raceway maximum compressive stress, σ_{Mol}, N/cm^2	1.302×10^9	1.5306×10^9	1.740×10^9	2.046×10^9	1.600×10^9	1.764×10^9	1.948×10^9	2.144×10^9
Right outer-raceway maximum compressive stress, σ_{Mor}, N/cm^2								

TABLE 2. - CHARACTERISTICS OF AN ARCH BEARING, g = 0.254 MM (0.010 IN.), FOR AN AXIAL APPLIED LOAD OF 4448 N (1000 LB) AND 22 241 N (5000 LB)

[Inner-raceway groove curvature, 0.54; outer raceway groove curvature, 0.52; pitch diameter, 187.55 mm (7.3838 in.); ball diameter, 22.23 mm (0.8750 in.); diametral play, 0.2499 mm (0.0098 in.); 22 balls.]

Rotational speed of inner raceway, n_i, rpm	Axially applied load, F_a, 4448 N (1000 lb)				Axially applied load, F_a, 22 241 N (5000 lb)			
	12 000	16 000	20 000	24 000	12 000	16 000	20 000	24 000
Life, L, hr	31 602	8368	2440	792	975	520	274	124
Inner-raceway load, Q_r, N	389.8	422.1	491.4	671.2	2040	2112	2320	2837
Left-outer raceway load, Q_{ol}, N	1288	1807	2452	3257	3111	3834	4571	5490
Right-outer raceway load, Q_{or}, N	5350	1093	1798	2651	452.8	730.6	1469	2557
Inner-raceway contact angle, β_r, deg	28.52	25.76	21.65	15.34	30.21	27.47	23.80	18.63
Left-outer raceway contact angle, β_{ol}, deg	17.25	16.96	16.70	16.48	18.93	19.02	18.60	18.07
Right-outer raceway contact angle, β_{or}, deg	15.37	15.44	15.48	15.46	13.39	13.13	13.33	13.59
Inner-raceway spin to roll ratio, ω_{cr}/ω_{Ri}	0.5806	0.4966	0.3978	0.2705	0.5182	0.5542	0.4604	0.3314
Left-outer raceway spin to roll ratio, $\omega_{Sol}/\omega_{Rol}$	0.3493	0.3206	0.3010	0.2908	0.2759	0.3821	0.3588	0.3192
Right-outer raceway spin to roll ratio, $\omega_{Sor}/\omega_{Ror}$	-0.2377	-0.2611	-0.2760	-0.2815	-0.2037	-0.1988	-0.2160	-0.2486
Cage to shaft speed ratio, Ω_c/Ω_i	0.4639	0.4543	0.4458	0.4367	0.4661	0.4606	0.4490	0.4388
Inner-raceway maximum compressive stress, σ_{Mi}, N/cm^2	0.9887×10^9	1.016×10^9	1.071×10^9	1.191×10^9	1.717×10^9	1.737×10^9	1.795×10^9	1.924×10^9
Left outer-raceway maximum compressive stress, σ_{Mor}, N/cm^2	1.158×10^9	1.296×10^9	1.435×10^9	1.577×10^9	1.554×10^9	1.666×10^9	1.766×10^9	1.877×10^9
Right outer-raceway maximum compressive stress, σ_{Mor}, N/cm^2	0.8632×10^9	1.096×10^9	1.293×10^9	1.472×10^9	0.8163×10^9	0.9577×10^9	1.209×10^9	1.453×10^9

TABLE 3. - CHARACTERISTICS OF AN ARCH BEARING, g = 0.381 MM (0.015 IN.), FOR AN AXIAL APPLIED LOAD OF 4448 N (1000 LB) and 22 241 N (5000 LB)

[Inner-raceway groove curvature, 0.54; outer raceway groove curvature, 0.52; pitch diameter, 187.55 mm (7.3838 in.); ball diameter, 22.23 mm (0.8750 in.); diametral play, 0.2499 mm (0.0098 in.); 22 balls.]

Rotational speed of inner raceway, n_i, rpm	Axially applied load, F_a, 4448 N (1000 lb)				Axially applied load, F_a, 22 241 N (5000 lb)			
	12 000	16 000	20 000	24 000	12 000	16 000	20 000	24 000
Life, L, hr	35 072	7972	2195	709	1185	621	277	114
Inner-raceway load, Q_r, N	404.3	447.1	525.0	119.3	1902	2044	2393	2980
Left-outer raceway load, Q_{ol}, N	1174	1738	2431	3266	2834	3432	4265	5335
Right-outer raceway load, Q_{or}, N	701.0	1280	1983	2827	437.6	1087	2050	3175
Inner-raceway contact angle, β_r, deg	28.65	25.94	21.91	15.77	30.13	27.66	24.21	19.25
Left-outer raceway contact angle, β_{ol}, deg	25.27	25.03	24.81	24.59	26.35	25.94	25.50	25.14
Right-outer raceway contact angle, β_{or}, deg	28.65	24.43	24.29	24.13	23.11	23.17	23.18	23.10
Inner-raceway spin to roll ratio, ω_{cr}/ω_{Ri}	0.5445	0.4836	0.3998	0.2803	0.6122	0.5239	0.4424	0.3416
Left-outer raceway spin to roll ratio, $\omega_{Sol}/\omega_{Rol}$	0.4701	0.4635	0.4590	0.4545	0.5318	0.4862	0.4677	0.4589
Right-outer raceway spin to roll ratio, $\omega_{Sor}/\omega_{Ror}$	-0.4585	-0.4576	-0.4544	-0.4508	-0.3930	-0.4281	-0.4372	-0.4366
Cage to shaft speed ratio, Ω_c/Ω_i	0.4530	0.4464	0.4378	0.4278	0.4547	0.4476	0.4412	0.4322
Inner-raceway maximum compressive stress, σ_{Mi}, N/cm^2	1.000×10^9	1.036×10^9	1.095×10^9	1.218×10^9	1.675×10^9	1.718×10^9	1.813×10^9	1.955×10^9
Left outer-raceway maximum compressive stress, σ_{Mol}, N/cm^2	1.125×10^9	1.282×10^9	1.434×10^9	1.582×10^9	1.510×10^9	1.609×10^9	1.730×10^9	1.864×10^9
Right outer-raceway maximum compressive stress, σ_{Mor}, N/cm^2	1.000×10^9	1.158×10^9	1.340×10^9	1.507×10^9	0.8094×10^9	1.096×10^9	1.354×10^9	1.566×10^9

TABLE 4. - CHARACTERISTICS OF AN ARCH BEARING, g = 0.508 MM (0.020 IN.), FOR AN AXIAL APPLIED LOAD OF 4448 N (1000 LB) AND 22 241 N (5000 LB)

[Inner-raceway groove curvature, 0.54; outer raceway groove curvature, 0.52; pitch diameter, 187.55 mm (7.3838 in.); ball diameter, 22.23 mm (0.8750 in.); diametral play, 0.2499 mm (0.0098 in.); 22 balls.]

Rotational speed of inner raceway, n_i, rpm	Axially applied load, F_a, 4448 N (1000 lb)				Axially applied load, F_a, 22 241 N (5000 lb)			
	12 000	16 000	20 000	24 000	12 000	16 000	20 000	24 000
Life, L, hr	32 838	7487	2073	677	1154	595	280	116
Inner-raceway load, Q_r, N	414.8	450.0	552.1	700.1	1959	2105	2375	2916
Left-outer raceway load, Q_{ol}, N	1146	1709	2399	3229	2653	3296	4128	5211
Right-outer raceway load, Q_{or}, N	793.6	1357	2048	2878	890.5	1538	2381	3474
Inner-raceway contact angle, β_r, deg	28.81	26.14	22.18	16.18	30.49	28.05	24.58	19.72
Left-outer raceway contact angle, β_{ol}, deg	34.32	34.05	33.77	33.48	34.59	34.27	33.92	33.55
Right-outer raceway contact angle, β_{or}, deg	33.95	33.73	33.49	33.23	33.05	32.89	32.68	32.43
Inner-raceway spin to roll ratio, ω_{cr}/ω_{Ri}	0.5466	0.4879	0.4054	0.2881	0.5756	0.5213	0.4474	0.3498
Left-outer raceway spin to roll ratio, $\omega_{Sol}/\omega_{Rol}$	0.6782	0.6717	0.6650	0.6581	0.6719	0.6650	0.6575	0.6495
Right-outer raceway spin to roll ratio, $\omega_{Sor}/\omega_{Ror}$	-0.6778	-0.6717	-0.6652	-0.6584	-0.6680	-0.6626	-0.6563	-0.6486
Cage to shaft speed ratio, Ω_c/Ω_i	0.4330	0.4265	0.4183	0.4087	0.4370	0.4308	0.4231	0.4143
Inner-raceway maximum compressive stress, σ_{Mi}, N/cm^2	1.009×10^9	1.038×10^9	1.093×10^9	1.207×10^9	1.692×10^9	1.735×10^9	1.808×10^9	1.941×10^9
Left outer-raceway maximum compressive stress, σ_{Mol}, N/cm^2	1.120×10^9	1.280×10^9	1.433×10^9	1.587×10^9	1.482×10^9	1.593×10^9	1.717×10^9	1.855×10^9
Right outer-raceway maximum compressive stress, σ_{Mor}, N/cm^2	0.9908×10^9	1.185×10^9	1.359×10^9	1.522×10^9	1.029×10^9	1.235×10^9	1.429×10^9	1.620×10^9

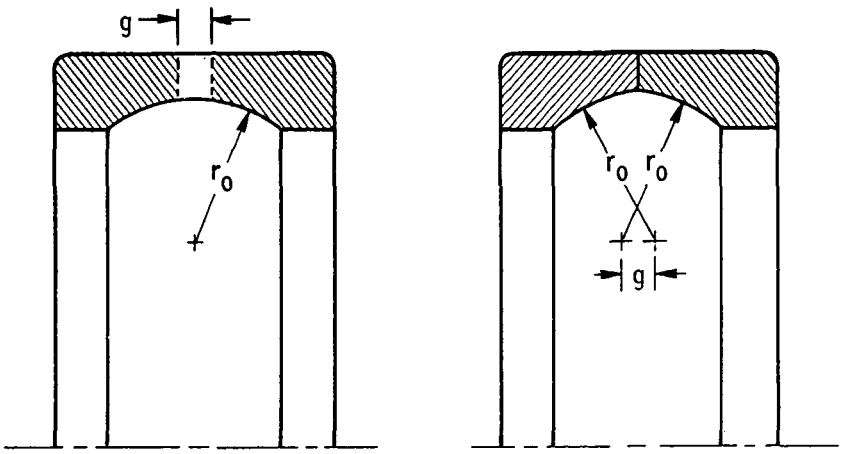

(a) Conventional. (b) Arched.

Figure 1. - Bearing outer race geometries.

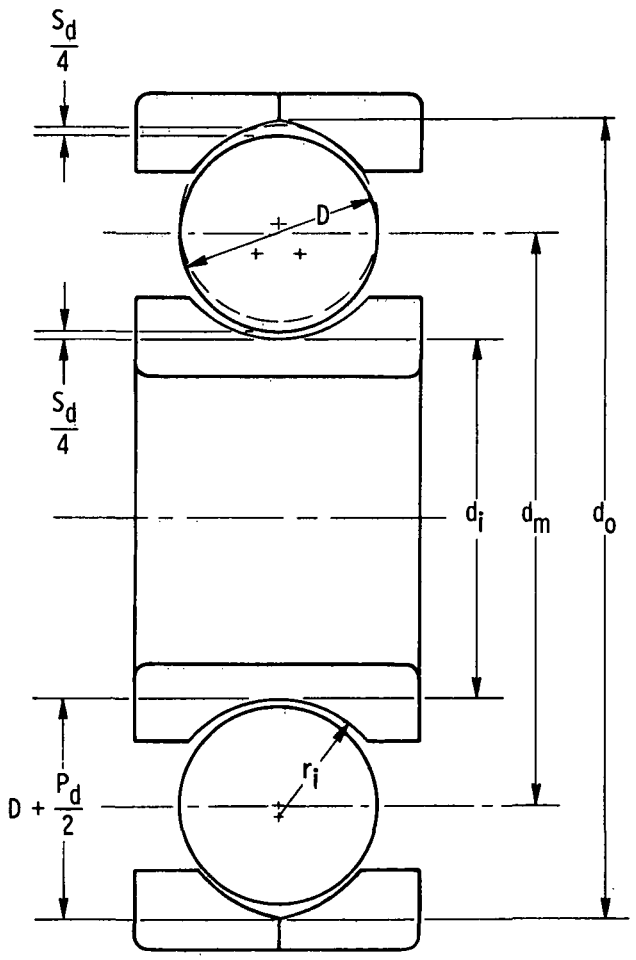

Figure 2. - Arched ball bearing in noncontacting position.

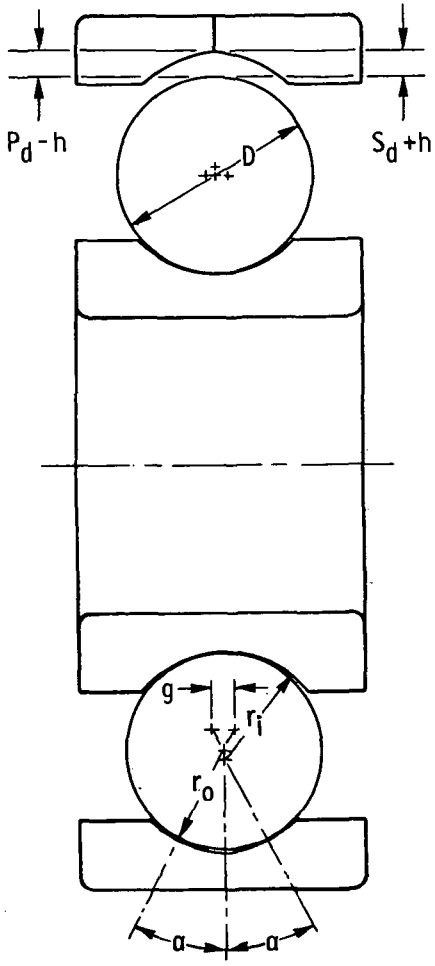

(a) Radial contact position.

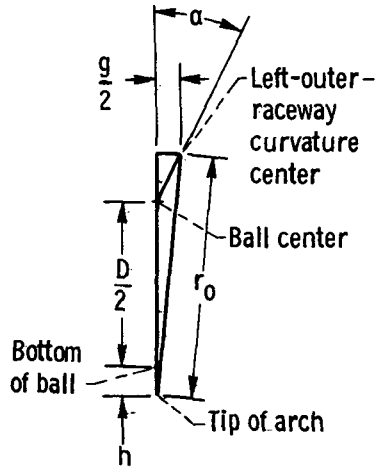

(b) Details of contact.

Figure 3. - Arched ball bearing radially loaded.

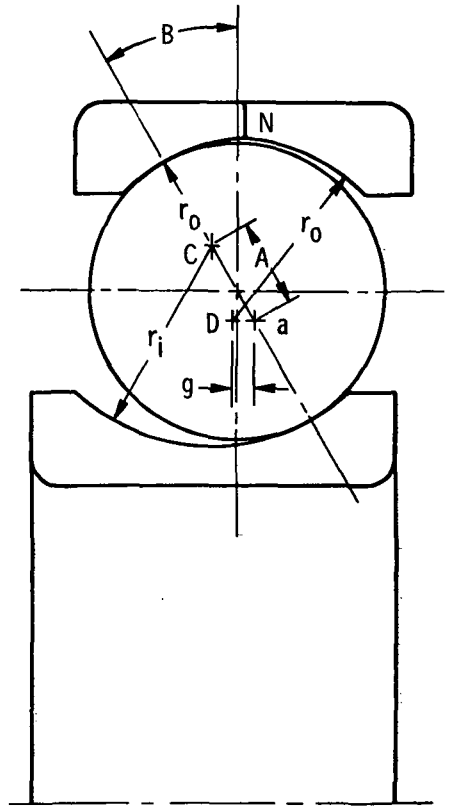

(b) Axial contact position of top ball.

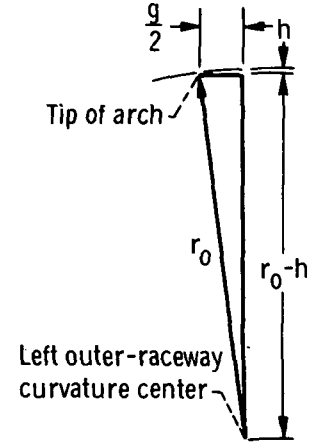

(a) Details of contact.

Figure 4. - Arched ball bearing axially loaded.

$\mathscr{A}$ Left-side outer-race curvature center
$\mathscr{B}$ Ball center, initial
$\mathscr{C}$ Inner-raceway curvature center, initial
$\mathscr{D}$ Right-side outer-race curvature center
$\mathscr{L}$ Ball center, final
$\mathscr{M}$ Inner-raceway groove curvature center, final

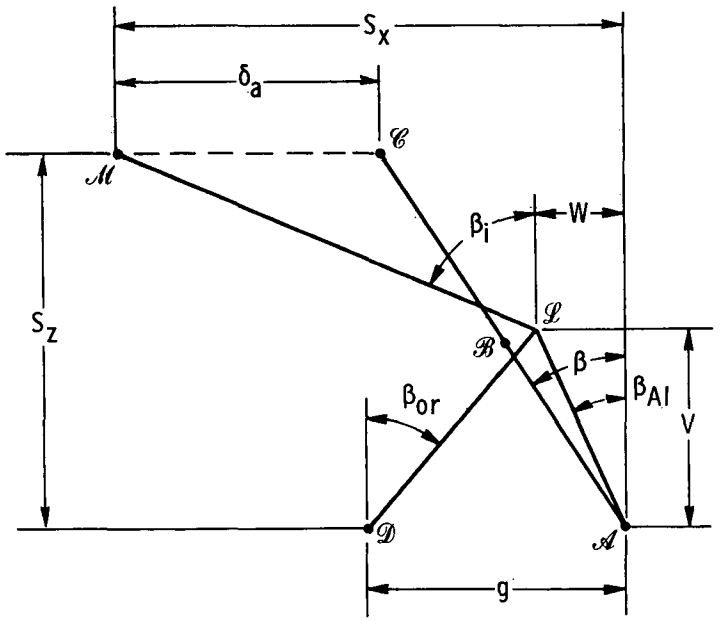

Figure 5. - Position of ball center and raceway groove curvature centers with and without centrifugal force acting on ball. Points shown for ball in top position, with bearing loaded axially.

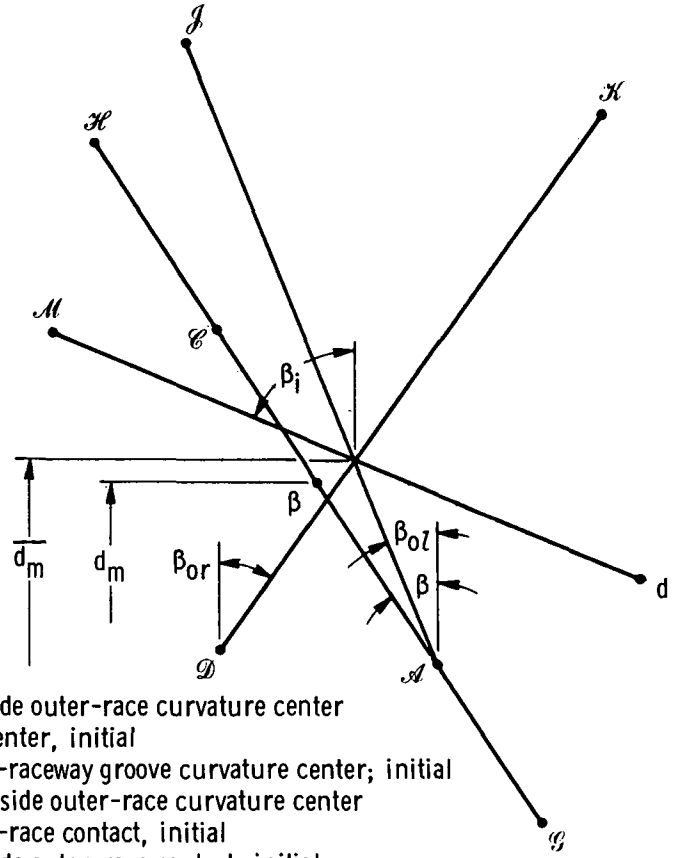

$\mathscr{A}$ Left-side outer-race curvature center
$\mathscr{B}$ Ball center, initial
$\mathscr{C}$ Inner-raceway groove curvature center; initial
$\mathscr{D}$ Right-side outer-race curvature center
$\mathscr{G}$ Inner-race contact, initial
$\mathscr{H}$ Left-side outer-race contact, initial
$\mathscr{I}$ Inner-race contact, final
$\mathscr{J}$ Left-side outer-race contact, final
$\mathscr{K}$ Right-side outer-race contact, final
$\mathscr{L}$ Ball center, final
$\mathscr{M}$ Inner-raceway groove,curvature center, final

Figure 6. - Position of ball and raceway groove curvature centers and contacts with and without force acting on ball.

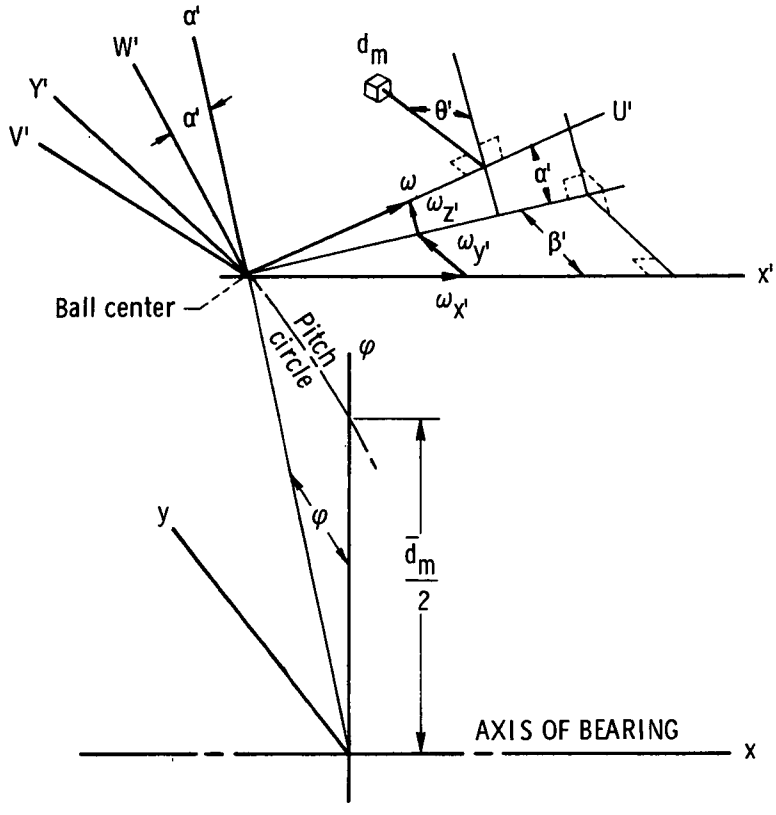

Figure 7. - Instantaneous position of element of mass in ball.

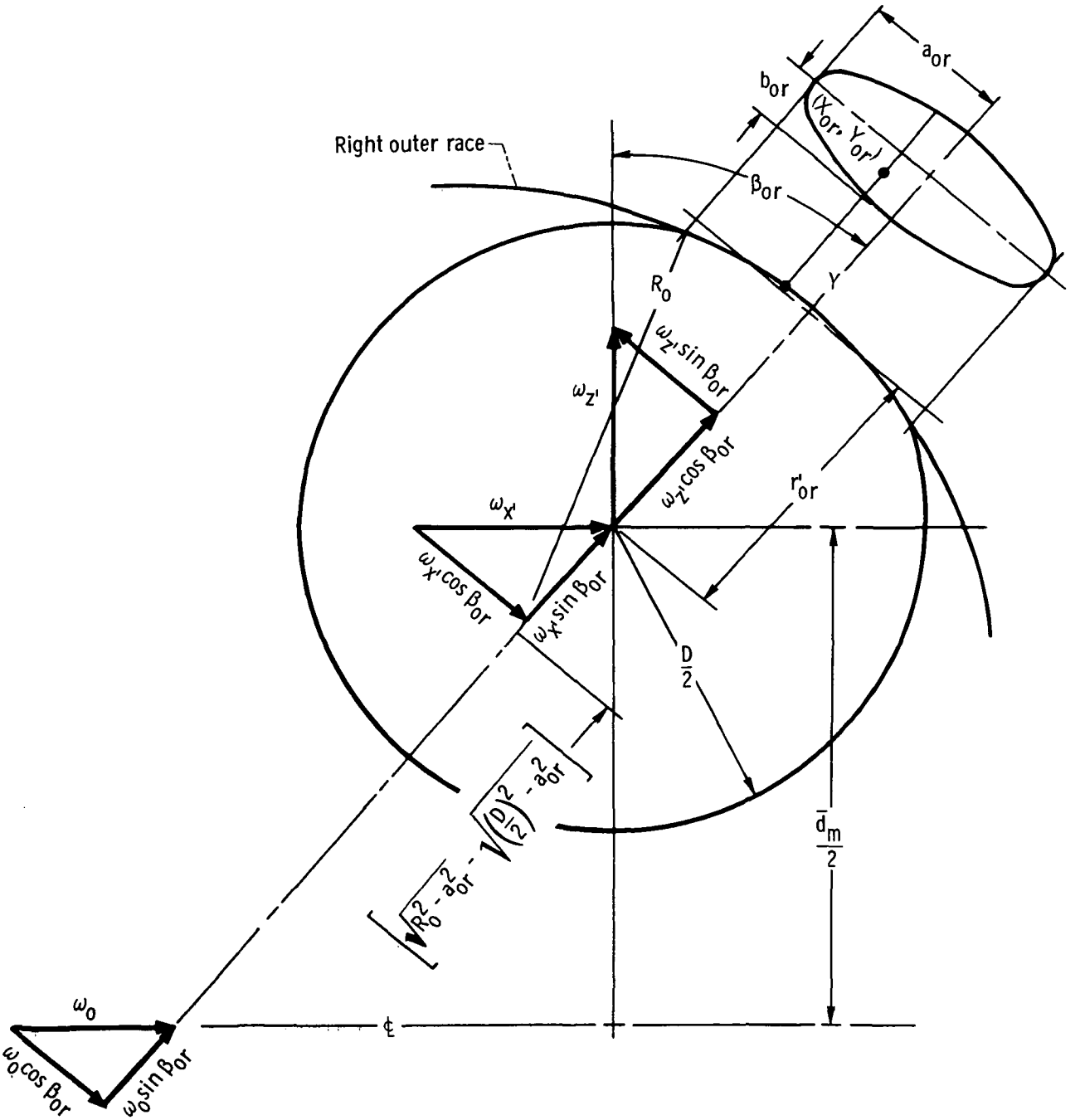

Figure 8. - Contact of ball with right outer race.

E-7607

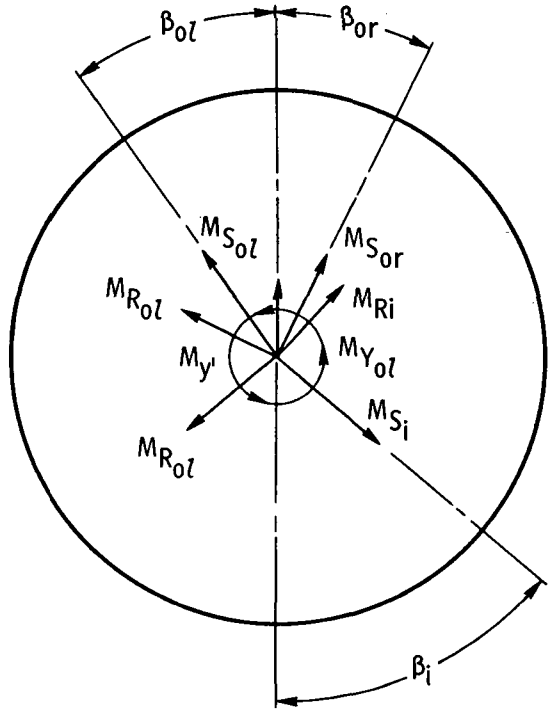

Figure 9. - Moments acting on ball.

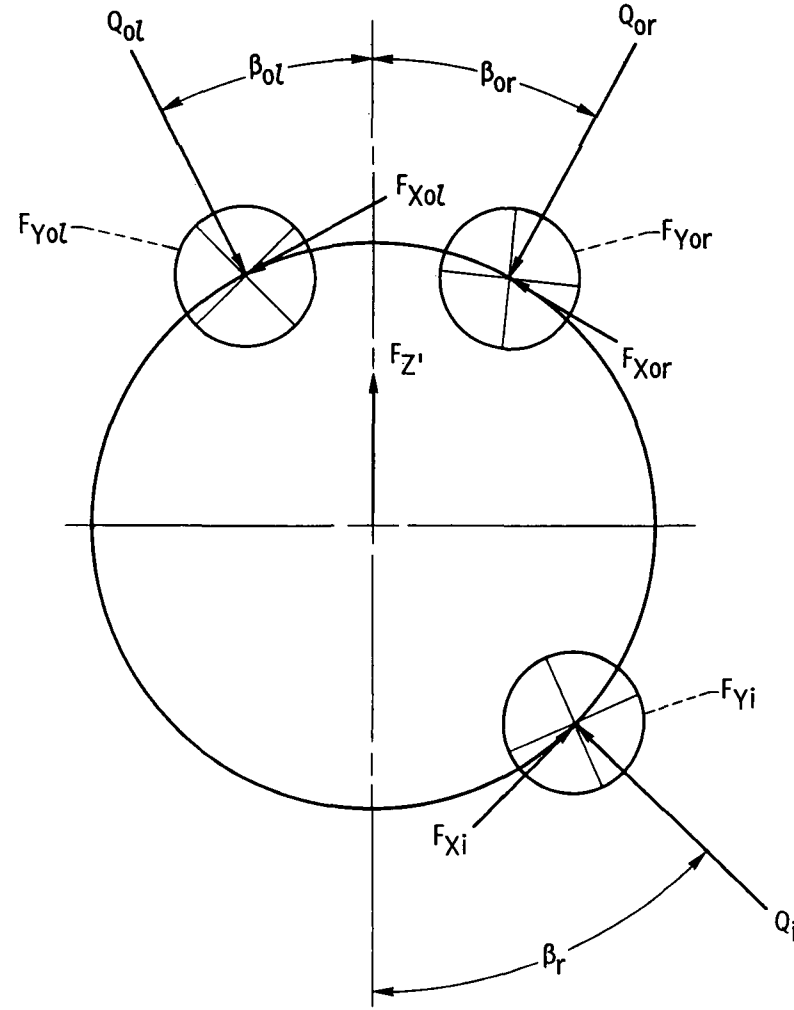

Figure 10. - Forces acting on ball.

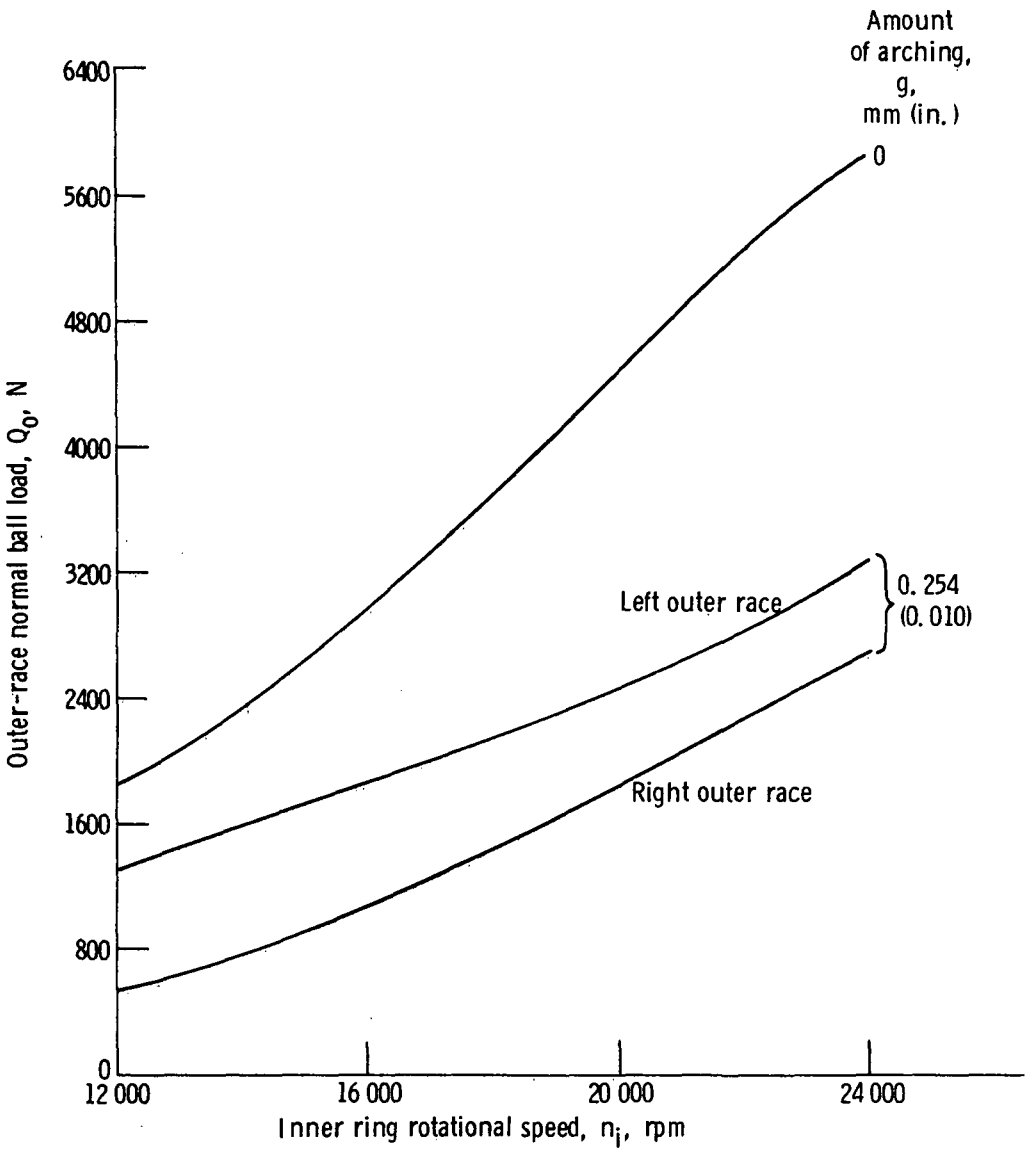

Figure 11. - Effect of speed on outer-race normal ball load, Q_o, for arched bearing (arching, 0.254 mm; 0.010 in.) and a conventional bearing (arching, 0) for a axial applied load of 4450 newtons (1000 lb).

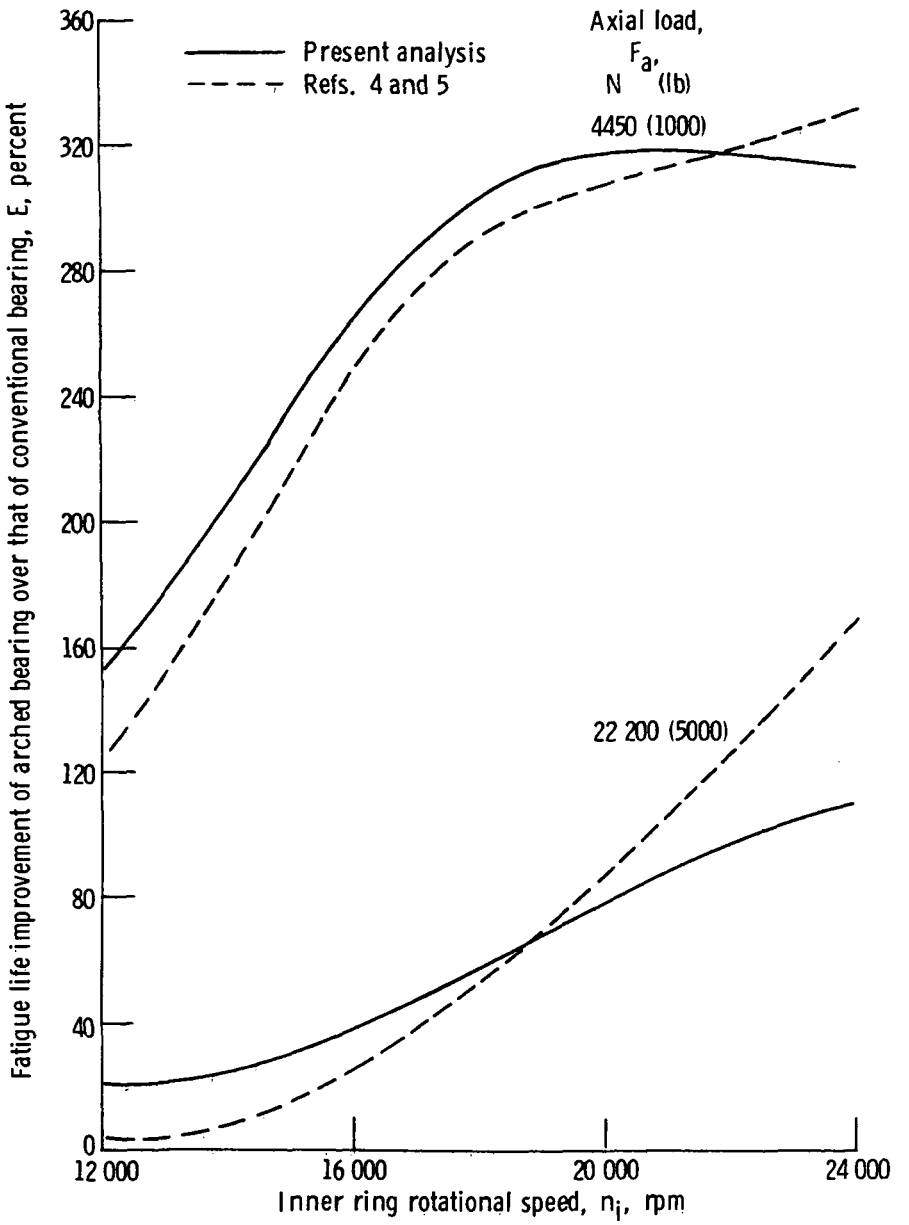

Figure 12. - Effect of speed on fatigue life percent improvement of arched bearing (arching, 0.254 mm; 0.010 in.) compared with that of conventional bearing for axially applied loads of 4450 newtons (1000 lb) and 22 200 newons (5000 lb).

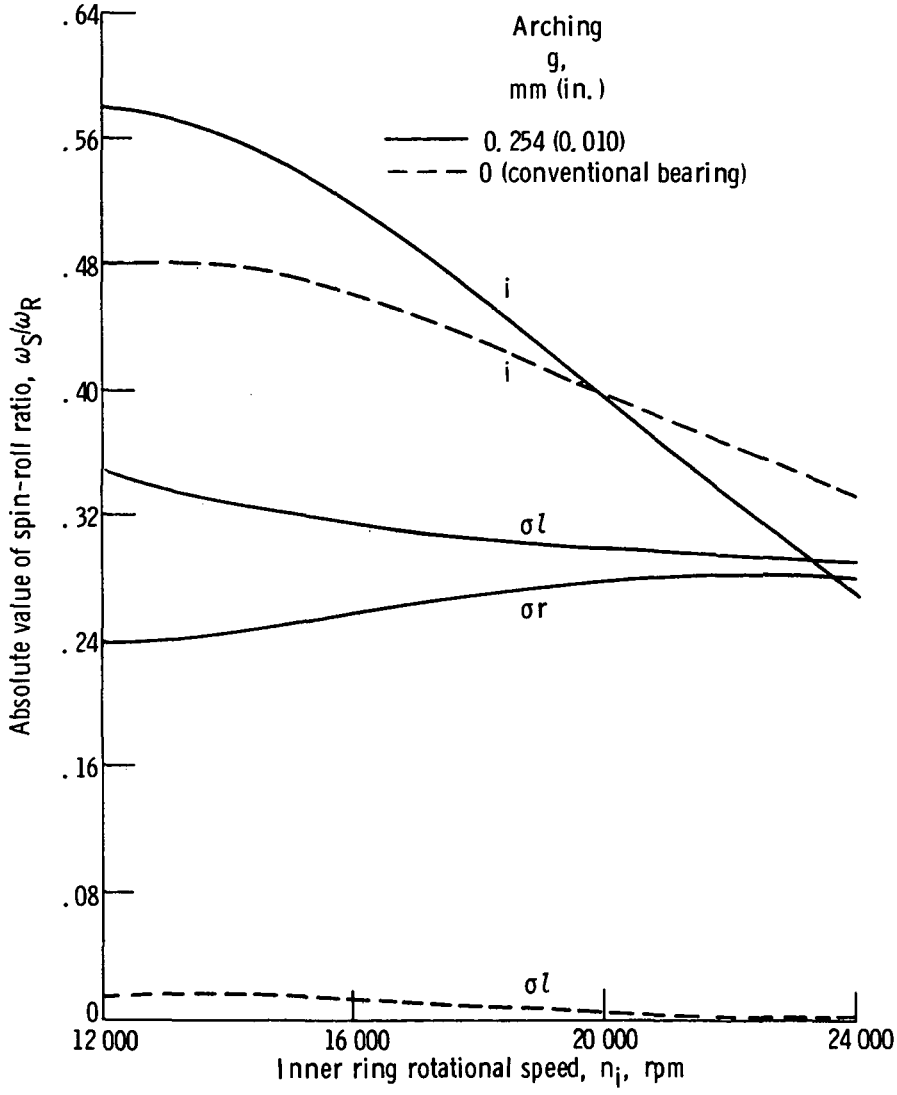

Figure 13. - Effect of speed on absolute value of spin to roll ratio for arch bearing and a conventional bearing for a axial applied load of 4450 newtons (1000 lb).